ervation of both types of information in the hippocampal output may form the basis of its key role in episodic memory (*2*, *34*).

References and Notes

1. J. O'Keefe, L. Nadel, *The Hippocampus as a Cognitive Map* (Clarendon, Oxford, 1978).
2. H. Eichenbaum, P. Dudchenko, E. Wood, M. Shapiro, H. Tanila, *Neuron* **23**, 209 (1999).
3. B. L. McNaughton, R. G. M. Morris, *Trends Neurosci.* **10**, 408 (1987).
4. J. O'Keefe, J. Dostrovsky, *Brain Res.* **34**, 171 (1971).
5. R. U. Muller, J. L. Kubie, J. B. Ranck, *J. Neurosci.* **7**, 1935 (1987).
6. B. L. McNaughton, C. A. Barnes, J. O'Keefe, *Exp. Brain Res.* **52**, 41 (1983).
7. J. J. Knierim, H. S. Kudrimoti, B. L. McNaughton, *J. Neurosci.* **15**, 1648 (1995).
8. J. O'Keefe, D. H. Conway, *Exp. Brain Res.* **31**, 573 (1978).
9. K. M. Gothard, W. E. Skaggs, B. L. McNaughton, *J. Neurosci.* **16**, 8027 (1996).
10. M. L. Shapiro, H. Tanila, H. Eichenbaum, *Hippocampus* **7**, 624 (1997).
11. E. R. Wood, P. A. Dudchenko, H. Eichenbaum, *Nature* **397**, 613 (1999).
12. E. J. Markus *et al.*, *J. Neurosci.* **15**, 7079 (1995).
13. M. A. Moita, S. Rosis, Y. Zhou, J. E. LeDoux, H. T. Blair, *J. Neurosci.* **24**, 7015 (2004).
14. E. R. Wood, P. A. Dudchenko, R. J. Robitsek, H. Eichenbaum, *Neuron* **27**, 623 (2000).
15. J. Ferbinteanu, M. L. Shapiro, *Neuron* **40**, 1227 (2003).
16. M. R. Bower, D. R. Euston, B. L. McNaughton, *J. Neurosci.* **25**, 1313 (2005).
17. S. A. Hollup, S. Molden, J. G. Donnett, M.-B. Moser, E. I. Moser, *J. Neurosci.* **21**, 1635 (2001).
18. E. Bostock, R. U. Muller, J. L. Kubie, *Hippocampus* **1**, 193 (1991).
19. C. Kentros *et al.*, *Science* **280**, 2121 (1998).
20. A. Cressant, R. U. Muller, B. Poucet, *Exp. Brain Res.* **143**, 470 (2002).
21. D. Marr, *J. Physiol.* **202**, 437 (1969).
22. S. Leutgeb, J. K. Leutgeb, A. Treves, M.-B. Moser, E. I. Moser, *Science* **305**, 1295 (2004); published online 22 July 2004 (10.1126/science.1100265).
23. Materials and methods are available as supporting material on *Science* Online.
24. The mean number of pretraining days in the test environment was 17 (square-circle), 14 (two rooms), and 4 (black-white).
25. The rate threshold was 0.27 Hz. Similar results were obtained with rate thresholds of 0.10 Hz and 0.50 Hz (tables S1 and S2) (*23*).
26. K. M. Gothard, W. E. Skaggs, K. M. Moore, B. L. McNaughton, *J. Neurosci.* **16**, 823 (1996).
27. W. E. Skaggs, B. L. McNaughton, *J. Neurosci.* **18**, 8455 (1998).
28. H. Tanila, *Hippocampus* **9**, 235 (1999).
29. If the external spatial input is strong enough, it is theoretically possible for large changes to occur in the firing rates of some cells, whereas intrinsic attractor dynamics of the network maintain the relative relations between the place fields of the ensemble (*35*).
30. S. A. Hollup, S. Molden, J. G. Donnett, M.-B. Moser, E. I. Moser, *Eur. J. Neurosci.* **13**, 1197 (2001).
31. In these studies, which all focused on CA1, much of the residual activity in the less active condition appeared inside the cell's place field in the more active condition [e.g., figure 8 in (*30*), figures 3 to 5 in (*14*), figures 2 to 6 in (*15*), figure 6 in (*16*), figures 6B and 9 in (*12*), and figure 4 in (*13*)], as expected if the remapping was primarily rate-based. In (*30*), 70% of the cells exhibited peak activity in the same quadrant in the two directions.
32. T. J. Wills, C. Lever, F. Cacucci, N. Burgess, J. O'Keefe, *Science* **308**, 873 (2005).
33. H. Markram, M. Tsodyks, *Nature* **382**, 807 (1996).
34. E. Tulving, *Annu. Rev. Psychol.* **53**, 1 (2002).
35. A. Samsonovich, B. L. McNaughton, *J. Neurosci.* **17**, 5900 (1997).

36. We thank R. G. M. Morris and M. P. Witter for discussion and A. M. Amundsgård, I. M. F. Hammer, K. Haugen, K. Jenssen, R. Skjerpeng, E. Sjulstad, B. H. Solem, and H. Waade for technical assistance. The work was supported by a Centre of Excellence grant from the Norwegian Research Council.

Supporting Online Material

www.sciencemag.org/cgi/content/full/309/5734/619/DC1
Materials and Methods
Figs. S1 to S5
Tables S1 and S2

25 April 2005; accepted 10 June 2005
10.1126/science.1114037

Complete Replication of Hepatitis C Virus in Cell Culture

Brett D. Lindenbach,[1] Matthew J. Evans,[1] Andrew J. Syder,[1] Benno Wölk,[1] Timothy L. Tellinghuisen,[1] Christopher C. Liu,[2] Toshiaki Maruyama,[3]* Richard O. Hynes,[2] Dennis R. Burton,[3] Jane A. McKeating,[1]† Charles M. Rice[1]‡

Many aspects of the hepatitis C virus (HCV) life cycle have not been reproduced in cell culture, which has slowed research progress on this important human pathogen. Here, we describe a full-length HCV genome that replicates and produces virus particles that are infectious in cell culture (HCVcc). Replication of HCVcc was robust, producing nearly 10^5 infectious units per milliliter within 48 hours. Virus particles were filterable and neutralized with a monoclonal antibody against the viral glycoprotein E2. Viral entry was dependent on cellular expression of a putative HCV receptor, CD81. HCVcc replication was inhibited by interferon-α and by several HCV-specific antiviral compounds, suggesting that this in vitro system will aid in the search for improved antivirals.

HCV is a major cause of chronic liver disease, with over 170 million persistently infected individuals worldwide (*1*). HCV-associated liver disease frequently progresses to cirrhosis, which can lead to liver failure and hepatocellular carcinoma. Current drug therapies are often poorly tolerated and effective in only a fraction of patients; there is no vaccine for HCV. A major obstacle to understanding the virus life cycle and to developing improved therapeutics is the inability to efficiently grow HCV in cell culture.

HCV is an enveloped, positive-sense RNA virus of the family *Flaviviridae*. Naturally occurring variants of HCV are classified into six major genotypes. The 9.6-kb genome encodes one large polyprotein that is processed by viral and cellular proteinases to produce the virion structural proteins (core and glycoproteins E1 and E2) as well as nonstructural (NS) proteins (p7 through NS5B) (Fig. 1A). Subgenomic RNA replicons have been adapted for efficient RNA replication in the human hepatoma line Huh-7 and other cultured cells (*2*–*5*). However, full-length genomes containing cell culture–adaptive mutations do not produce infectious virus particles in culture and are severely attenuated in vivo (*6*–*8*). This led us to hypothesize that mutations that enhance RNA replication may have deleterious effects on virion production. To test this idea, we used a genotype 2a subgenomic replicon, SGR-JFH1, that efficiently replicates in cell culture without adaptive mutations (*4*). Full-length chimeric genomes were constructed with the use of the core-NS2 gene regions from the infectious J6 (genotype 2a) and H77 (genotype 1a) virus strains (Fig. 1A). Both full-length chimeras and the subgenomic RNA were competent for RNA replication, as seen by the accumulation of NS5A protein and viral RNA 48 hours after RNA transfection into the Huh-7.5 cell line (Fig. 1B). As expected, mutation of the NS5B RNA polymerase active site [GlyAspAsp to GlyAsnAsp (GND)] destroyed the ability of FL-J6/JFH to replicate (Fig. 1B). Within transfected cells, both full-length genomes expressed core, E2, and NS5A (Fig. 1C). As expected, SGR-JFH1 expressed NS5A but not core or E2. While ≈30% of cells were productively transfected with FL-J6/JFH, FL-H77/JFH, or SGR-JFH1 RNA (Fig. 1B), >95% of FL-J6/JFH–transfected cells were positive for NS5A by 96 hours (fig. S1). This suggested that FL-J6/JFH spread within the transfected cell cultures.

To test whether infectivity could be transferred to naïve cells, we clarified conditioned

[1]Center for the Study of Hepatitis C, The Rockefeller University, 1230 York Avenue, New York, NY 10021, USA. [2]Howard Hughes Medical Institute, Center for Cancer Research, Massachusetts Institute of Technology, Cambridge, MA 02139, USA. [3]Departments of Immunology and Molecular Biology, The Scripps Research Institute, La Jolla, CA 92037, USA.

*Present address: Alexion Antibody Technologies, San Diego, CA 92121, USA.
†Present address: Division of Immunity and Infection, Institute of Biomedical Research, University of Birmingham Medical School, Birmingham B15 2TT, UK.
‡To whom correspondence should be addressed. E-mail: ricec@rockefeller.edu

media from these cultures by centrifugation (*9*), filtered the supernatants (0.2 μm), and incubated them with naïve Huh-7.5 cells. NS5A expression could be transferred by the FL-J6/JFH–transfected culture media but not by media from cells transfected with FL-H77/JFH or SGR-JFH1 (Fig. 1B). Interestingly, the amount of FL-J6/JFH RNA released into the transfected cell culture media exceeded that of the other RNAs by a factor of >200, and only FL-J6/JFH produced an extracellular form of core (Fig. 1C, lower panel). Given that the infectivity of the genotype 2a chimera is filterable and is associated with the release of HCV RNA and core protein, we refer to this cell culture–produced virus as HCVcc. The ability of the genotype 1a/2a chimera to replicate but not spread suggests that interactions between the structural and nonstructural gene products may be important for HCVcc formation, as has been observed for other members of this virus family (*10*, *11*).

Limiting dilution assays for NS5A expression in electroporated cells showed that 30.3 ± 9.5% (n = 6) of cells were productively transfected with FL-J6/JFH, and of these, 55% produced infectivity that was detectable upon transfer to naïve cells. Thus, FL-J6/JFH RNA transcripts were highly infectious and formation of HCVcc did not depend on the emergence of rare variants. Limiting dilution assays were also used to quantitate the amount of HCVcc infectivity between samples as median tissue culture infectious units per milliliter ($TCID_{50}$/ml). The $TCID_{50}$ is the dilution that infects 50% of replicate cell cultures (*9*). After an eclipse phase (≥9 hours), FL-J6/JFH infectivity could be detected in the media by 18 hours posttransfection, and it continued to accumulate until 48 hours (Fig. 1D). Interestingly, FL-J6/JFH (H2476L), which contained a weakly adaptive mutation in NS5B (*4*), showed slightly delayed growth kinetics but also peaked to similar levels by 48 hours. Viruses could be serially passaged, infecting 50 to 90% of cells within 5 days after two rounds of passage at a low multiplicity of infection (MOI) of 0.1 to 1.0 (Fig. 1E). The expression and subcellular localization of core, E2, and NS5A within FL-J6/JFH–infected cells was consistent with what was previously seen in full-length and subgenomic replicon-bearing cells [supporting online material (SOM) text]. Taken together, these measurements show that HCVcc replication is robust and occurs with kinetics similar to those of other *Flaviviridae*.

A classic method in virus identification is to neutralize the suspected virus with specific antisera. As shown in Fig. 2A, an E2-specific human monoclonal antibody neutralized HCVcc infectivity in a dose-dependent manner, whereas an isotype-matched control antibody had no effect on HCVcc titer. These data affirm the viral nature of HCVcc infectivity and show that E2 is essential for virus entry.

HCV E2 has been shown to bind to the cellular surface protein CD81 (*12*), which is an essential coreceptor for the entry of HCV glycoprotein-pseudotyped retroviruses (*13*–*15*). We found that HCVcc infectivity could be blocked with a soluble recombinant form of the CD81 large extracellular loop (Fig. 2B).

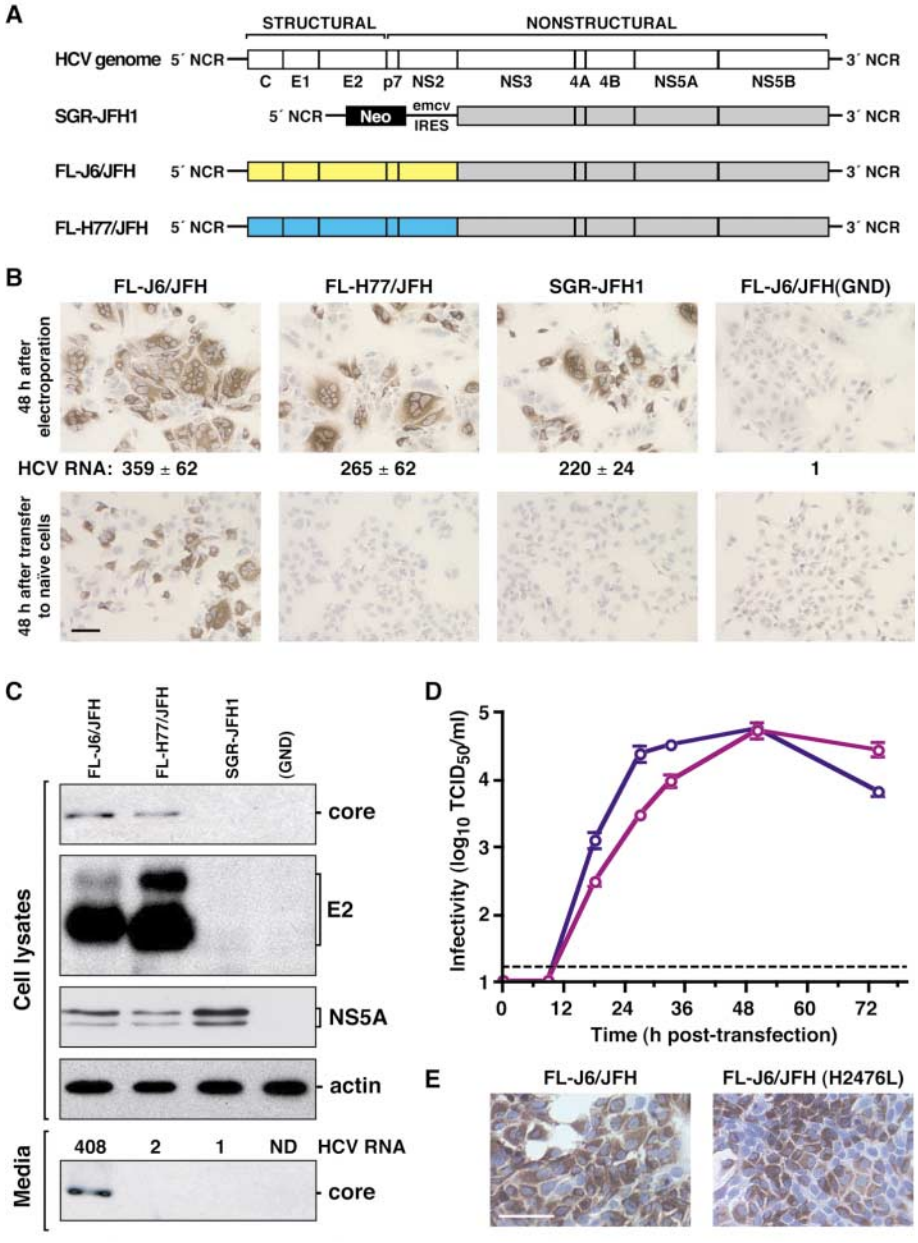

Fig. 1. Production of infectious HCV in cell culture. (**A**) The structures of the HCV RNA genome, the SGR-JFH1 replicon, and full-length chimeric genomes FL-J6/JFH and FL-H77/JFH. NCR, noncoding region; C, core; yellow, J6; cyan, H77. (**B**) Huh-7.5 cells were electroporated with RNA transcripts of the indicated genomes [or the RNA-polymerase defective mutant FL-J6/JFH(GND)] 48 hours before immunostaining for NS5A (brown, upper panel). Nuclei were counterstained with hematoxylin (blue). Below is the relative amount of HCV RNA detected in each transfected cell population at 48 hours by quantitative reverse transcription polymerase chain reaction (RT-PCR). Naïve Huh-7.5 cells were incubated for 48 hours with filtered, conditioned media from the transfected cells and immunostained for NS5A expression (lower panel). (**C**) Western blot for HCV core, E2, NS5A, or actin protein expression at 48 hours in RNA transfected Huh-7.5 cells. Below each lane is the relative amount of HCV RNA and core detected in cell culture media by quantitative RT-PCR and Western blot, respectively. ND, not determined. (**D**) The accumulation of HCVcc infectivity after electroporation of FL-J6/JFH (blue) or FL-J6/JFH (H2476L) (purple) into 6 × 10^5 cells/timepoint, assessed by a limiting dilution assay (mean ± SEM; n = 4). Dotted line, assay sensitivity. (**E**) Cells were immunostained for NS5A 5 days after infection with serially passaged virus. Scale bars, 100 μm.

To further examine the role of CD81 in virus entry we used HepG2 cells, which lack CD81 expression but are capable of supporting HCV RNA replication (*3*). As seen in Fig. 2C, normal HepG2 cells were not infected by FL-J6/JFH, whereas CD81-expressing HepG2 cells were infected under the same conditions, albeit with reduced efficiency (≈850 times less than Huh-7.5 cells). These data confirm that interactions between E2 and CD81 are important for HCV entry.

The physical nature of HCV particles has been difficult to study in the absence of an infectious culture system. In density gradients, clinical isolates of HCV exhibit a broad distribution and unusually low buoyant densities [reviewed in (*16*)]. These properties have been partly explained by the interaction of HCV with serum components such as immunoglobulins and β-lipoproteins. We examined the profiles of RNA and infectivity associated with HCVcc particles by equilibrium centrifugation in 10 to 40% iodixanol, an iso-osmotic gradient material. A series of controls confirmed that this method accurately measured the buoyant density of HCVcc (SOM text). HCV RNA was broadly distributed through the top of the gradient, with a peak in fractions 16 and 17 (1.13 to 1.14 g/ml), and was not found beyond fraction 20 (1.18 g/ml) (Fig. 3A). HCVcc infectivity was also broadly distributed among fractions 1 to 15 (1.01 to 1.12 g/ml), and infectivity was not seen beyond fraction 18 (1.17 g/ml). Surprisingly, fractions 16 and 17, which contained the highest levels of HCV RNA, had little infectivity associated with them. The specific infectivity of a virus preparation relates the amount of infectivity to the total number of virus particles or genomes in the preparation. Interestingly, a plot of HCVcc-specific infectivity versus buoyant density indicates that the most infectious material is at 1.09 to 1.10 g/ml (Fig. 3B), which is similar to the peak of infectivity (1.09 to 1.11 g/ml) previously seen in chimpanzees (*17*). In contrast, RNA-containing material with a buoyant density of 1.14 g/ml (fraction 17) had a low specific infectivity, with ≈300,000 RNA molecules per infectious unit. Many groups have reported an HCV RNA peak near this density (*18*–*20*), although infectivity could not be assessed.

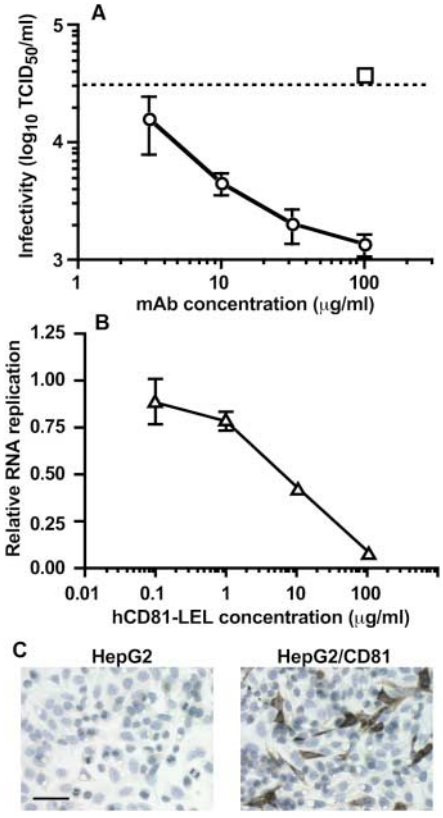

Fig. 2. HCVcc infection is dependent on HCV glycoprotein functions. (**A**) FL-J6/JFH (H2476L) was pre-incubated for 1 hour at 37°C with the indicated concentrations of recombinant human anti-E2 C1 (circles) or anti-dengue virus NS1 (square) immunoglobulin G1 monoclonal antibodies (mAb), then titered by limiting dilution assay (mean ± SEM; $n = 3$). Assays for both antibodies were conducted in parallel. The dotted line indicates the titer of untreated virus. (**B**) FL-J6/JFH (H2476L) was preincubated with 12 μg/ml of a recombinant form of the large extracellular loop (LEL) of CD81 and used to infect naïve cells. The levels of HCV RNA, relative to an untreated control, were determined at 48 hours postinfection by quantitative RT-PCR (mean ± SEM; $n = 4$). (**C**) HepG2 or HepG2/CD81 cells were infected with FL-J6/JFH for 48 hours before immunostaining for NS5A expression. Scale bar, 100 μm.

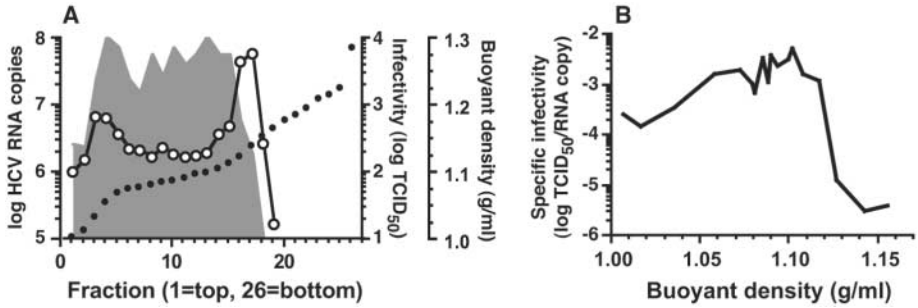

Fig. 3. Characterization of HCVcc particles. (**A**) The profiles of FL-J6/JFH (H2476L) RNA (open circles) and infectivity (solid gray) are shown after isopycnic centrifugation in a 10 to 40% iodixanol gradient. Closed circles indicate the buoyant density of each fraction. (**B**) The specific infectivity of each fraction in panel (A) was calculated as the infectivity per RNA copy and plotted against the buoyant density.

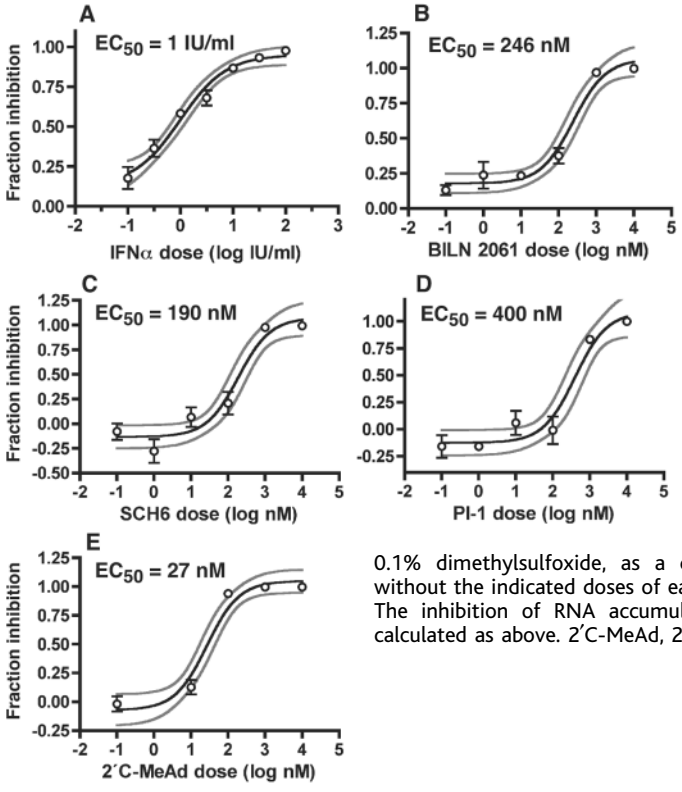

Fig. 4. Antiviral inhibition of HCVcc. (**A**) Huh-7.5 cells were incubated for 18 hours with the indicated doses of IFN before infection with FL-J6/JFH (H2476L) (MOI of 1.0). The fraction of inhibition was calculated from the levels of HCV RNA at 48 hours postinfection. The mean ± SEM ($n = 3$), best-fit curve (black), and 95% confidence interval (gray curves) are shown. (**B** to **E**) After 8 hours inoculation with FL-J6/JFH (H2476L) (MOI of 0.1), Huh-7.5 cells were washed and incubated in media containing 0.1% dimethylsulfoxide, as a carrier control, with or without the indicated doses of each anti-HCV compound. The inhibition of RNA accumulation at 48 hours was calculated as above. 2′C-MeAd, 2′C-methyladenosine.

Thus, HCVcc exhibits physical properties similar to those that have been previously described for natural isolates of HCV.

There is an urgent need for improved HCV drug therapies. The current standard treatment, pegylated interferon-α (IFNα) and ribavirin, leads to a sustained response in only ≈50% of genotype 1–infected patients. We examined the ability of HCVcc replication to be inhibited by IFNα and other antiviral compounds. Dose-response experiments showed that IFNα inhibited HCVcc RNA accumulation in infected cells with a median effective concentration (EC_{50}) of 1 international unit (IU)/ml (Fig. 4A). We also tested three HCV-specific inhibitors of the NS3 serine protease for their effects on HCVcc infection. As seen in Fig. 4, B to D, BILN 2061 (*21*), SCH6 (*22*), and PI-1 (*23*) all inhibited HCVcc RNA accumulation in the submicromolar range. In addition, a nucleoside analog inhibitor of the NS5B RNA polymerase, 2′C-methyladenosine (*24*), was found to inhibit HCVcc replication in the low nanomolar range (Fig. 4E). Thus, HCVcc infection can be inhibited by IFNα and several HCV-specific antiviral compounds. The specificity of these latter compounds further shows that HCVcc infection leads to authentic replication in target cells and demonstrates that this infectious system may be useful for testing current and future antiviral compounds.

We describe a full-length genotype 2a HCV genome that replicates and produces virus particles that are infectious in cell culture. This system lays a foundation for future in vitro studies to examine new aspects of the virus life cycle and to develop new drugs for combating HCV.

Note added in proof: Full-length JFH-1 has also been recently reported to produce infectious virus in cell culture (*25–27*), as has a genotype 1b Com1/JFH-1 chimera (*28*), albeit with lower efficiency and slower growth kinetics than the system reported here.

References and Notes

1. Anonymous, *Wkly. Epidemiol. Rec.* **75**, 18 (2000).
2. K. J. Blight, A. A. Kolykhalov, C. M. Rice, *Science* **290**, 1972 (2000).
3. T. Date *et al.*, *J. Biol. Chem.* **279**, 22371 (2004).
4. T. Kato *et al.*, *Gastroenterology* **125**, 1808 (2003).
5. V. Lohmann *et al.*, *Science* **285**, 110 (1999).
6. K. J. Blight, J. A. McKeating, C. M. Rice, *J. Virol.* **76**, 13001 (2002).
7. J. Bukh *et al.*, *Proc. Natl. Acad. Sci. U.S.A.* **99**, 14416 (2002).
8. T. Pietschmann *et al.*, *J. Virol.* **76**, 4008 (2002).
9. Materials and methods are available as supporting material on *Science* Online.
10. E. V. Agapov *et al.*, *J. Virol.* **78**, 2414 (2004).
11. B. M. Kümmerer, C. M. Rice, *J. Virol.* **76**, 4773 (2002).
12. P. Pileri *et al.*, *Science* **282**, 938 (1998).
13. B. Bartosch *et al.*, *J. Biol. Chem.* **278**, 41624 (2003).
14. E. G. Cormier *et al.*, *Proc. Natl. Acad. Sci. U.S.A.* **101**, 7270 (2004).
15. J. Zhang *et al.*, *J. Virol.* **78**, 1448 (2004).
16. R. Bartenschlager, M. Frese, T. Pietschmann, *Adv. Virus Res.* **63**, 71 (2004).
17. D. Bradley *et al.*, *J. Med. Virol.* **34**, 206 (1991).
18. N. Fujita *et al.*, *J. Med. Virol.* **63**, 108 (2001).
19. T. Heller *et al.*, *Proc. Natl. Acad. Sci. U.S.A.* **102**, 2579 (2005).
20. M. Hijikata *et al.*, *J. Virol.* **67**, 1953 (1993).
21. D. Lamarre *et al.*, *Nature* **426**, 186 (2003).
22. A. K. Saksena *et al.*, International Patent Application WO 02/008244 (2002).
23. K. Lin, A. D. Kwong, C. Lin, *Antimicrob. Agents Chemother.* **48**, 4784 (2004).
24. S. S. Carroll *et al.*, *J. Biol. Chem.* **278**, 11979 (2003).
25. T. Wakita, T. Kato, T. Date, M. Miyamoto, paper presented at the 11th International Symposium on HCV and Related Viruses, Heidelberg, Germany, 5 October 2004.
26. T. Wakita *et al.*, *Nat. Med.* 12 June 2005 (10.1038/nm1268).
27. J. Zhong *et al.*, *Proc. Natl. Acad. Sci. U.S.A.* 6 June 2005 (10.1073/pnas.0503596102).
28. T. Pietschmann *et al.*, paper presented at the 11th International Symposium on HCV and Related Viruses, Heidelberg, Germany, 5 October 2004.

29. We thank P. Holst, V. Kramer, and N. Torres for technical assistance; J. Bloom, A. Gauthier, L. Dustin, and D. Bernard for careful review of the manuscript; T. Wakita for SGR-JFH1, SGR-JFH (H2476L), and SGR-JFH(GND); J. Bukh for pJ6CF; D. Moradpour for C7-50 antibody; T. von Hahn and J. Zhang for HepG2/CD81 cells; Boehringer Ingelheim for BILN 2061; The Schering-Plough Research Institute for SCH6; C. Lin and A. Kwong of Vertex Pharmaceutical, Inc. for PI-1; and D. Olsen and S. Ludmerer at Merck for 2′C-methyladenosine. Funded by grants from NIH (CA57973, CA85883, AI40034 to C.M.R., CA10702 to B.D.L., DK70497 to A.J.S., AI51820 to T.L.T., AI50798 to J.A.M.) and the Greenberg Medical Research Institute. Additional support was provided by the Charles H. Revson Foundation (M.J.E.) and the German Science Foundation (Deutsche Forschungsgemeinschaft) (B.W.). B.D.L. is a recipient of the National Cancer Institute Howard Temin Award. C.M.R. is a manager of and has equity in Apath, LLC, which has an exclusive license for the Huh-7.5 cell line.

Supporting Online Material
www.sciencemag.org/cgi/content/full/1114016/DC1
Materials and Methods
SOM Text
Figs. S1 to S3
References and Notes

25 April 2005; accepted 31 May 2005
Published online 9 June 2005;
10.1126/science.1114016
Include this information when citing this paper.

Genome-Scale Identification of Nucleosome Positions in *S. cerevisiae*

Guo-Cheng Yuan, Yuen-Jong Liu,* Michael F. Dion, Michael D. Slack,† Lani F. Wu, Steven J. Altschuler, Oliver J. Rando‡

The positioning of nucleosomes along chromatin has been implicated in the regulation of gene expression in eukaryotic cells, because packaging DNA into nucleosomes affects sequence accessibility. We developed a tiled microarray approach to identify at high resolution the translational positions of 2278 nucleosomes over 482 kilobases of *Saccharomyces cerevisiae* DNA, including almost all of chromosome III and 223 additional regulatory regions. The majority of the nucleosomes identified were well-positioned. We found a stereotyped chromatin organization at Pol II promoters consisting of a nucleosome-free region ~200 base pairs upstream of the start codon flanked on both sides by positioned nucleosomes. The nucleosome-free sequences were evolutionarily conserved and were enriched in poly-deoxyadenosine or poly-deoxythymidine sequences. Most occupied transcription factor binding motifs were devoid of nucleosomes, strongly suggesting that nucleosome positioning is a global determinant of transcription factor access.

Nucleosomes prevent many DNA binding proteins from approaching their sites (*1–3*), whereas appropriately positioned nucleosomes can bring distant DNA sequences into close proximity to promote transcription (*4*). Current understanding of the primary structure of chromatin and its effects on gene expression comes from a handful of well-characterized loci (see examples below). High-resolution measurements of nucleosome positions over chromosome-scale distances would enhance our understanding of chromatin structure and function.

To measure nucleosome positions on a genomic scale, we developed a DNA microarray method (*5*) to identify nucleosomal and linker DNA sequences on the basis of susceptibility of linker DNA to micrococcal nuclease (fig. S1). Nucleosomal DNA was isolated, labeled with Cy3 fluorescent dye (green), and mixed with Cy5-labeled total genomic DNA (red). This mixture was hybridized to microarrays printed with overlapping 50-mer oligonucleotide probes tiled every 20 base pairs across chromosomal regions of interest (fig.

Bauer Center for Genomics Research, Harvard University, 7 Divinity Avenue, Cambridge, MA 02138, USA.

*Present address: Department of Molecular Biophysics and Biochemistry, Yale University, Post Office Box 208114, New Haven, CT 06520, USA.
†Present address: BAE Systems Advanced Information Technologies, 9655 Granite Ridge Drive, San Diego, CA 92123, USA.
‡To whom correspondence should be addressed. E-mail: orando@cgr.harvard.edu